Fuel 348 (2023) 128554

Contents lists available at ScienceDirect

Fuel

journal homepage: www.elsevier.com/locate/fuel

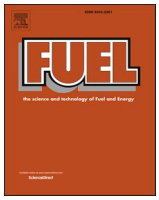

CO_2 capture as bicarbonate using DMAPA with incorporation of surface activity

Omar A. Carrasco-Jaim [b], Haojun Xia [a], Upali P. Weerasooriya [a], Ryosuke Okuno [a,*]

[a] Hildebrand Department of Petroleum and Geosystems Engineering, The University of Texas at Austin, Austin, TX 78712, United States
[b] McKetta Department of Chemical Engineering, The University of Texas at Austin, Austin, TX 78712, United States

ARTICLE INFO

Keywords:
CO_2 capture
CO_2 absorption
Amine
DMAPA
Surfactant
Bicarbonate

ABSTRACT

We present for the first time the CO_2 capture and *in-situ* conversion into bicarbonate as a carbon-bearing product using an amine with built-in surface activity. The surface-active amine was 3-(dimethylamino)propylamine (DMAPA) modified with propylene oxide (PO) groups (DMAPA-xPO, x = 4, 6, 8, 12). Analysis of the CO_2 capture capacity data with ^{13}C Nuclear Magnetic Resonance (NMR) spectroscopy determined the bicarbonate concentrations and the generation mechanism during the CO_2 capture influenced by the PO groups, establishing a relationship between CO_2 solubility, pH of the solution, and steric effect. Results demonstrated the effectiveness of the built-in surface activity with an optimal PO level (DMAPA-6PO). DMAPA-6PO enhanced the bicarbonate generation by 54%, in comparison to DMAPA, under ambient conditions.

1. Introduction

The current energy demands depend mainly on fossil fuels, such as coal, oil, and natural gas. The chemical energy extracted from them by combustion is broadly used for transportation, electricity generation, industrial processes, and heating. Their emitted pollutants are causing adverse effects on the environment and human health. In particular, carbon dioxide (CO_2) is one of the greenhouse gases and 92.4% of CO_2 emissions were caused by fossil fuel combustion in the United States in 2019 [1,2].

Different routes can mitigate CO_2 emissions, such as reducing energy use, improving energy efficiency, shifting to low-carbon or even non-carbon energy processes, and implementing carbon capture and utilization (CCU) systems [2]. CCU into fuels and chemicals is considered a suitable option to stabilize atmospheric greenhouse gas concentrations in the energy transition [3,4]. Using emitted CO_2 gas as feedstock to manufacture value-added products provides not only environmental benefits, but also opportunities for chemical industries to develop new production methods.

Amine-based post-combustion capture (PCC) is a well-proven and commercially used technology for CO_2 capture in the petroleum sector, coal-fired power, and cement industries, with a CO_2 recovery rate up to 800 tons/day [5–7]. This process typically uses a single or a blend of reactive aqueous amine solutions to react chemically with CO_2 gas in an acid-base reaction. Then, the CO_2 gas is subsequently stripped from the amine solution at high temperatures (120–180°C), regenerating the solvent [5]. However, the regeneration step is considered the main drawback of this technology because of its high regeneration cost, approximately 70% of the total operating cost [8].

Different approaches have been made to reducing energy consumption in PCC. The most common strategy is the development of less energy-intensive capture solvents, which are mixtures of different amines or ionic liquids (IL) [9–15]. However, this approach still requires heating for CO_2 desorption and amine regeneration. The necessity of heating can be avoided when CO_2 is captured to yield a non-gaseous carbon species to be directly used as a feedstock, such as bicarbonate (HCO_3^-).

Capturing CO_2 in the form of bicarbonate can be an effective, practical, and stable way not only to store and deliver a CO_2-bearing product into the utilization unit, but also to overcome the CO_2 mass transfer limitation in aqueous carbon capture technologies because of the higher carbon concentration in saturated solution (3.3 M for saturated $KHCO_3$ compared with 0.033 M for saturated CO_2) [16]. For example, the energy requirement for capturing CO_2 into potassium bicarbonate, 1.0 MJ/100 mol CO_2, is lower than that for capturing CO_2 into potassium carbonate in the direct air capture (DAC) process, 1.3 MJ/100 mol CO_2 [17]. Therefore, the bicarbonate pathway as an alternative CO_2 capturing route has considerable potential for post-combustion

* Corresponding author.
E-mail address: okuno@austin.utexas.edu (R. Okuno).

https://doi.org/10.1016/j.fuel.2023.128554
Received 20 December 2022; Received in revised form 25 March 2023; Accepted 26 April 2023
Available online 4 May 2023

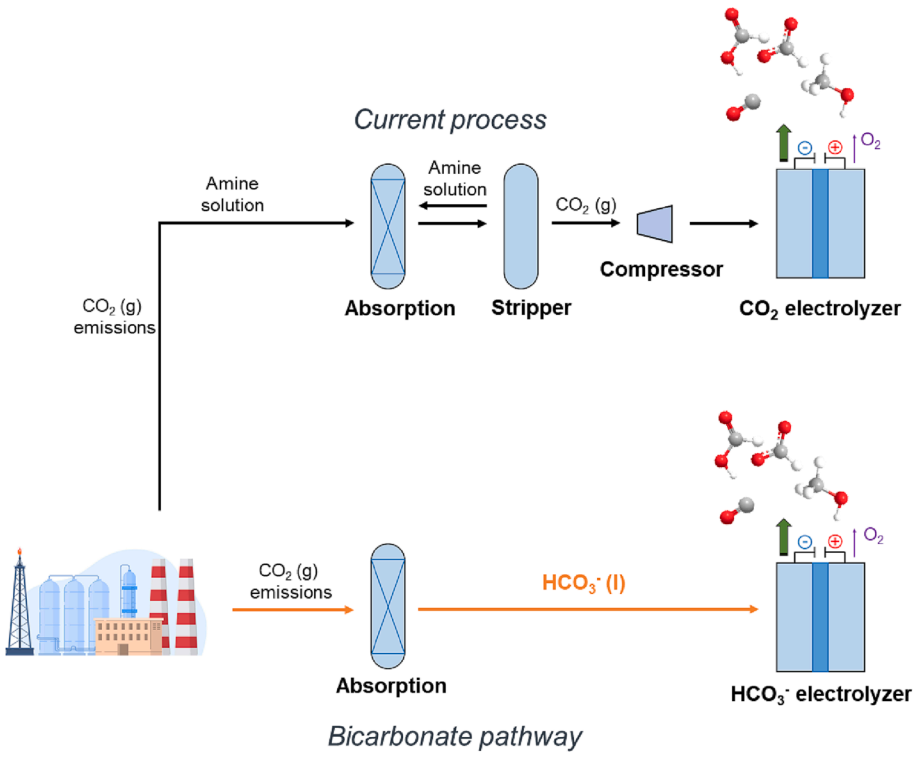

Scheme 1. Schematic representation of the proposed CO_2 capture into bicarbonate pathway for CCU technologies.

technology applications, and can be integrated into a conversion step such as electrochemical conversion to produce various chemicals and fuels, as shown in Scheme 1.

Tertiary amines react with CO_2 in a 1:1 mol ratio and produce bicarbonate with slow capture kinetics [18]. Although primary amines have demonstrated faster CO_2 capture kinetics than tertiary amines, they mainly produce carbamate ($R\text{-}NHCOO^-$) from this reaction [19,20]. Thus, a combined effect between a primary and tertiary amine is expected to improve the bicarbonate generation rate. For example, 3-(dimethylamino)propylamine or DMAPA, which is a diamine with one tertiary and one primary amino group, is a potential amine for this purpose. Even though DMAPA has been used as an experimental and simulation CO_2 capture solution model with analytical bicarbonate detection in the literature [21–23], it has not been studied for the bicarbonate generation as a CO_2 capture pathway or for the optimal experimental conditions for its production.

Additionally, surfactants have been studied to potentially enhance the CO_2 capture performance of different amine solutions since they lower their surface tension, increase the surface where CO_2 and amine react, and facilitate the CO_2 mass transfer into the aqueous solution [24–26]. In particular, low-concentration surfactants with short hydrophilic chains of less than ten carbons, such as ethylene oxide groups (EO), improved the CO_2 capture of monoethanolamine solutions (MEA) [27]. However, the effect of these surfactants was only studied when they were added to amine solutions without considering the bicarbonate generation [28,29]. To the best of our knowledge, no report has been published on incorporating surfactant characteristics into an amine for bicarbonate generation. Such amine species with built-in surface activity is referred to as surface-active amine in this research.

The envisioned applications of CO_2 capture as bicarbonate include an integrated CO_2 capture/conversion process via bicarbonate electrolysis as part of the potential pathways of carbon capture, utilization, and storage (CCUS). Since the bicarbonate product is not bonded to the surface-active amine (as carbamate), membrane technologies can cost-effectively separate bicarbonate because of their modular configuration, compactness, operational flexibility, and simplicity, as an alternative to the conventional thermal regeneration [30,31]. For instance, researchers have studied the direct electrolysis of the captured CO_2-

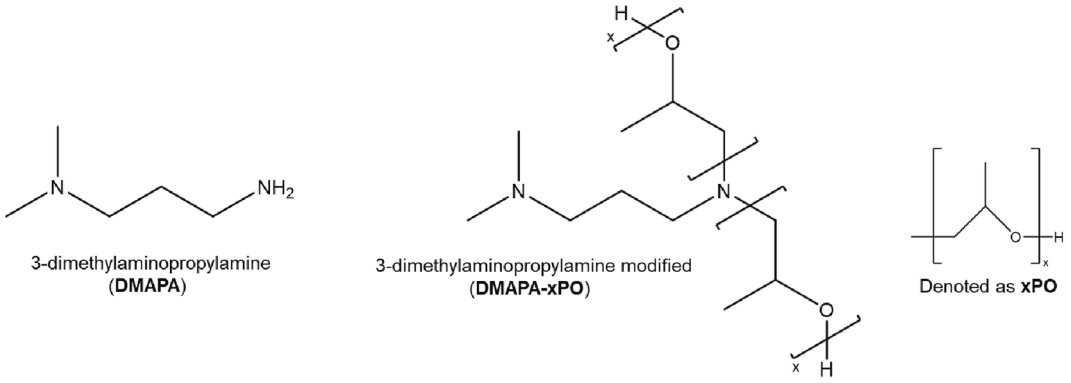

Scheme 2. Chemical structures of the amines used in this work.

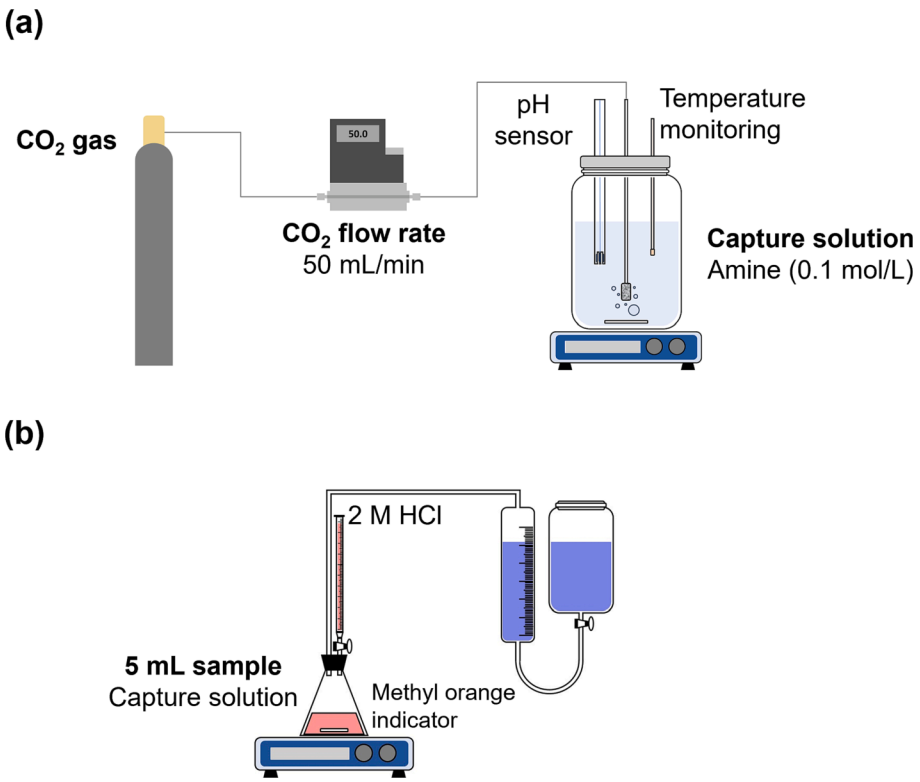

Scheme 3. Schematic representation of (a) CO_2 absorption experimental setup, and (b) CO_2 loading capacity determination.

amine solution, including MEA and AMP solutions, [32–34] and some surfactants in the media, such as CTAB [35]. Their studies indicated that CO_2 reduction can be negatively affected when such complex components in the electrolyte prevent CO_2 from reaching the electrocatalysts' active sites. Thus, the separation process can be an important step for the selective formation of the desired product in the bicarbonate pathway.

This paper reports an investigation of the CO_2 capture into bicarbonate using a surface-active amine as capturing solution. The surface-active amine was generated by attaching PO groups to DMAPA's primary amino group at different levels (DMAPA-xPO, x = 4, 6, 8, 12). The CO_2 capture capacity and the bicarbonate generation were analyzed by ^{13}C NMR spectroscopy. Results showed that surface-active amine with an optimal PO level (DMAPA-6PO) enhanced the bicarbonate concentration by approximately 54%, in comparison to DMAPA with no PO attached, because of enhanced CO_2 solubilization in the aqueous media.

2. Experimental

2.1. Chemicals

DMAPA and DMAPA-based surface-active amines (DMAPA-xPO) were provided by Harcros Chemicals. The carbon dioxide (CO_2) gas of an industrial grade (99.5%) was obtained from Linde Gas & Equipment Inc. Hydrochloric acid (HCl) 3 N and methyl orange indicator powder were purchased from Aqua Solutions and Thermo Scientific, respectively. All chemicals were used without further purification. Scheme 2 shows the chemical structure of the previously mentioned amines.

2.2. CO_2 capture experiments

The overall CO_2 capture performance was evaluated by (1) the CO_2 absorption capacity and (2) the CO_2 loading of the samples with the experimental setup shown in Scheme 3. For the CO_2 absorption capacity (Scheme 3a), a mass flow controller (FMA5508A-ST-CO_2 model by OMEGA Engineering Inc.) continuously supplied CO_2 gas at 50 mL/min into the capture solution in a glass reactor at room temperature. The solution was 600 mL of DMAPA or DMAPA-xPO (x = 4, 6, 8, and 12) with a concentration of 0.116 mol/L for all experiments. All solutions were prepared with deionized (DI) water (18.2 MΩ•cm resistivity). A stainless-steel sparger with a mean pore size of 2–10 μm was used as a nozzle tip for the CO_2 bubbling line. The temperature and pH were monitored during the tests using the Fisher Scientific Accumet AE150 pH meter. The absorption experiments were finished when the pH of the capture solution became constant. The amount of CO_2 absorbed by the capture solution was determined by measuring the mass of the solution before and after each test by using the Mettler Toledo ML104T analytical balance; hence, no samples were taken for measuring the CO_2 absorption capacity.

In a second run of each CO_2 absorption experiment under the same conditions, a 5 mL sample from the capture solution was taken every 10 min and placed into an Erlenmeyer flask for the CO_2 loading determination by titration using 2 M HCl solution and methyl orange as the indicator. Scheme 3b gives a schematic of the setup. During HCl addition, CO_2 gas was released upwards the glass tubing displacing the non-reactive solution mixture level (H_2SO_4, $NaHCO_3$, and NaCl) [27]. The CO_2 loading was calculated by using the following equation [36]:

$$\alpha_{CO2} = \frac{mol_{CO2}}{mol_{absorbent}} = \frac{\frac{P(V_{gas}-V_{HCl})}{RT}}{C_1 V_1} \quad (1)$$

where α_{CO2} is the CO_2 loading defined as mol of CO_2 captured per mole of absorbent, R denotes the gas constant (8.314 L kPa/mol K), P (kPa) and T (K) are the atmospheric pressure and temperature, respectively. C_1 (mol/L) and V_1 (mL) are the concentration and volume of the sample from the capture solution tested. The V_{gas} – V_{HCl} term represents the volume of the released CO_2 gas (mL) less the HCl volume used in the titration from the measured volume of the displaced liquid. Additionally, the CO_2 loading rate was calculated from the slope of the linear portion in the CO_2 loading history.

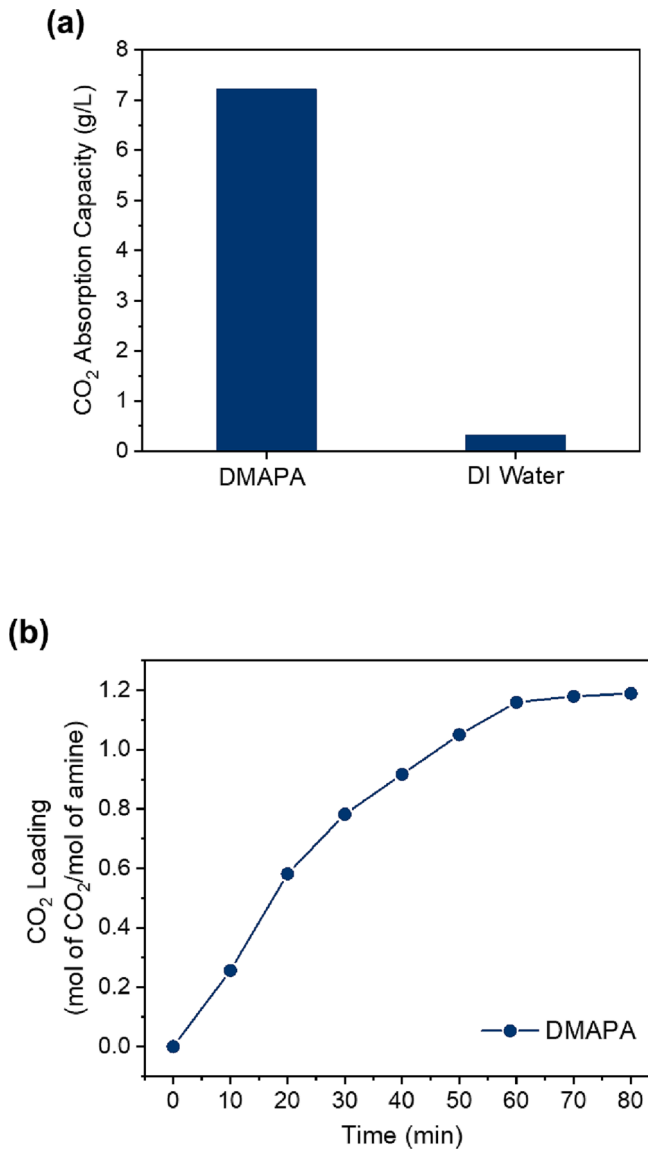

Fig. 1. (a) CO_2 capture capacity, and (b) CO_2 loading profile of 0.116 mol/L DMAPA.

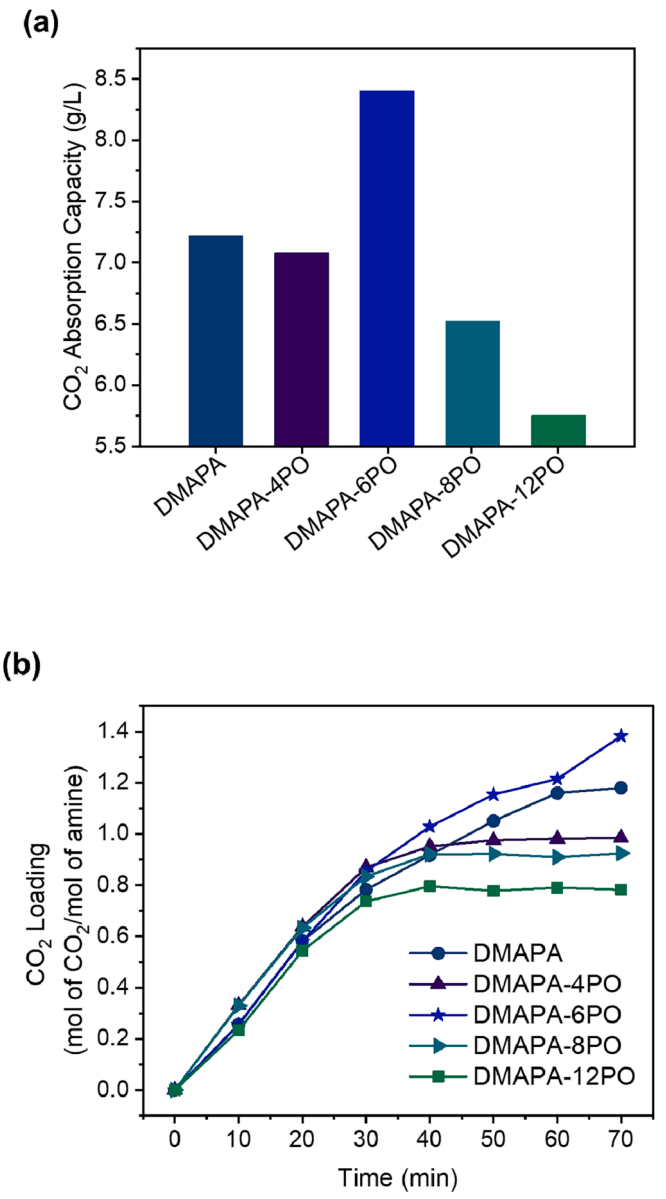

Fig. 2. (a) CO_2 absorption capacity, and (b) CO_2 loading profile of 0.116 mol/L DMAPA-xPO (x = 4, 6, 8, 12).

2.3. NMR analysis

^{13}C NMR spectroscopy was used to determine the carbon species generated from the CO_2 capture process, in particular, bicarbonate and carbamate. Therefore, 0.5 mL of the capture solution was collected and measured every 10 min during the absorption experiments. The samples were prepared with 100 μL of deuterium oxide (Thermo Scientific, for NMR 99.8 atom %D) to lock the system [37,38]. All analyses were carried out with a relaxation delay time of 2 s and a number of scans of 1024 using the Bruker Avance III 500 instrument. A calibration curve was used for the bicarbonate quantification. Thus, bicarbonate solutions of 0.05–3 mol/L concentration were prepared using potassium bicarbonate (Honeywell, ACS reagent ≥ 99.7%). Fig. S1 of Supporting information shows the obtained calibration curve. Alternatively, the quantification of carbamate was also estimated based on the following equation [38]:

$$m_a = m_b \frac{N_b}{N_a} \frac{A_a}{A_b} \frac{M_a}{M_b} \quad (2)$$

where N is the number of carbons related to the signal, A is the area under the NMR signal, M is the molecular weight, m_b is the mass of the reference material, and m_a is the mass of the analyte. As the reference, 0.02 g of tetramethylammonium chloride (Acros Organics, 98+%) was added during the sample preparation. The bicarbonate amount was also estimated by Eq. (2) and compared with NMR results, as listed in Table S1.

2.4. Surface tension measurements

Surface tensions were measured for amine solutions at room temperature by the CNC-DuNouy Interfacial Tensiometer (Cat. No. 70545) from CSC Scientific Company, Inc. The measurement range was 0–90 dynes/cm. A platinum-iridium ring of 6 cm circumference was used for the evaluations. Before each analysis, the ring was cleaned with soap, rinsed with isopropanol, and dried by air.

Table 1
Summarized results for the overall CO_2 capture performance of 0.116 mol/L DMAPA-xPO (x = 4, 6, 8, 12).

Sample	CO_2 Absorption[a] (g CO_2/L)	CO_2 Loading[b] (mol CO_2/mol amine)	CO_2 Loading Rate (min^{-1})
DMAPA	7.22	1.18	0.0212
DMAPA-4PO	7.08	0.98	0.0291
DMAPA-6PO	8.40	1.38	0.0265
DMAPA-8PO	6.52	0.92	0.0280
DMAPA-12PO	5.75	0.78	0.0252

[a] STD CO_2 absorption: ± 0.03; [b]STD CO_2 loading: ± 0.02.

3. Results

3.1. CO_2 capture performance of DMAPA and DMAPA-xPO

Firstly, the overall CO_2 capture performance of DMAPA without modification was evaluated. Fig. 1a shows the CO_2 absorption capacity. The mass of CO_2 absorbed by 0.116 mol/L DMAPA solution was 7.22 g/L, which was much greater than that by DI water, 0.33 g/L. The two amino groups present in DMAPA reacted with CO_2 through the zwitterion and the base-catalyzed hydration reactions [39,40], increasing the CO_2 solubility in the media, and therefore, the CO_2 absorption capacity [29]. During the absorption process, the pH of the solution decreased as a consequence of these acid-base reactions, as illustrated in Fig. S2a. The high initial value of 11.97 dropped to 7.20, which remained constant after 80 min of reaction.

The CO_2 loading history with DMAPA is shown in Fig. 1b. After the capture reaction started, the ratio of the CO_2 concentration to the amine concentrations increased to reach a maximum, 1.18 mol of CO_2/mol of amine, from 60 to 80 min. This loading capacity measured for DMAPA is in concordance with previously reported values, 1.05–1.35 mol of CO_2/mol of amine [23,41,42]. Additionally, the CO_2 loading rate was calculated to be 0.0212 min^{-1} from the CO_2 loading profile, as observed in Fig. S2b.

After having completed the performance of DMAPA as a reference sample, the amine with the built-in surface activity at different levels was evaluated as shown in Fig. 2. Among all the PO levels tested, DMAPA-6PO exhibited the highest CO_2 absorption capacity with 8.40 g/L, which was greater than DMAPA with no PO groups by 16%. PO levels lower (4PO) and higher (8PO and 12PO) than 6PO adversely affected the CO_2 capture capacity, underperforming DMAPA (see Fig. 2a). Thus, the built-in surface activity at the optimum level of 6PO allowed for a greater CO_2 dissolution, resulting in higher absorption capacity.

Moreover, the CO_2 loading profiles shown in Fig. 2b corroborated the absorption capacity tests. The optimum 6PO level exhibited the highest loading ratio of 1.38 mol of CO_2/mol of amine at 70 min of reaction. From this point on, the loading capacity was constant over an extended period (Fig. S3). The CO_2 capture kinetics was influenced by the different PO levels, in which an average rate of 0.0265 min^{-1} was greater than that of DMAPA (see Fig. S4). All results are summarized in Table 1. Overall, the built-in surface activity enabled DMAPA to increase the CO_2 capture kinetics, while significantly increasing the absorption capacity with the optimal PO level of six.

The CO_2 dissolution in the capture solution can play an important role in CO_2 capture. Therefore, the effect of PO groups on the surface tension of DMAPA-xPO solution was evaluated as presented in Fig. 3. The surface tension decreased with the PO level, starting at 42.9 dynes/cm for DMAPA-4PO to 37.1 dynes/cm for DMAPA-12PO, which were smaller than 67.6 dynes/cm for DMAPA by 36–45%. The reduction in surface tension likely caused a beneficial effect on the mass transfer rate [43], as shown by the enhanced rates of CO_2 loading capacity in Table 1. Fig. 3 also shows a correlation with the CO_2 loading rate. As the surface tension was reduced by the PO incorporation, the CO_2 loading rate increased up to 0.0291 min^{-1}, which was 37% greater than that of DMAPA. The PO group reduced the surface tension of DMAPA solution, and therefore increased the CO_2 dissolution kinetics.

Although DMAPA-12PO showed the smallest surface tension among those tested, it exhibited the worst performance of CO_2 capture. This observation can be associated with the surfactant properties of incorporated PO groups. A small hydrophobic head, such as propylene oxide (PO), exhibits high CO_2 affinity, resulting in a high CO_2 solubility because of a reduced repulsion in the aqueous media [29,30]. Simultaneously, the increasing steric hindrance because of the longer hydrocarbon chain in the increasing PO level negatively affects the CO_2

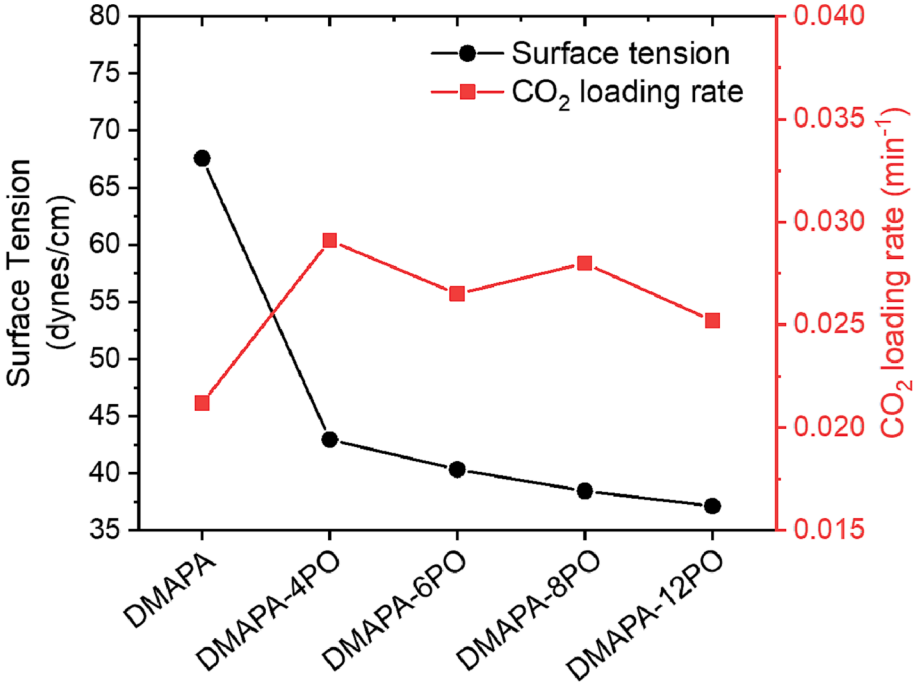

Fig. 3. PO group effects on surface tension and CO_2 loading rate of 0.116 mol/L DMAPA-xPO (x = 4, 6, 8, 12).

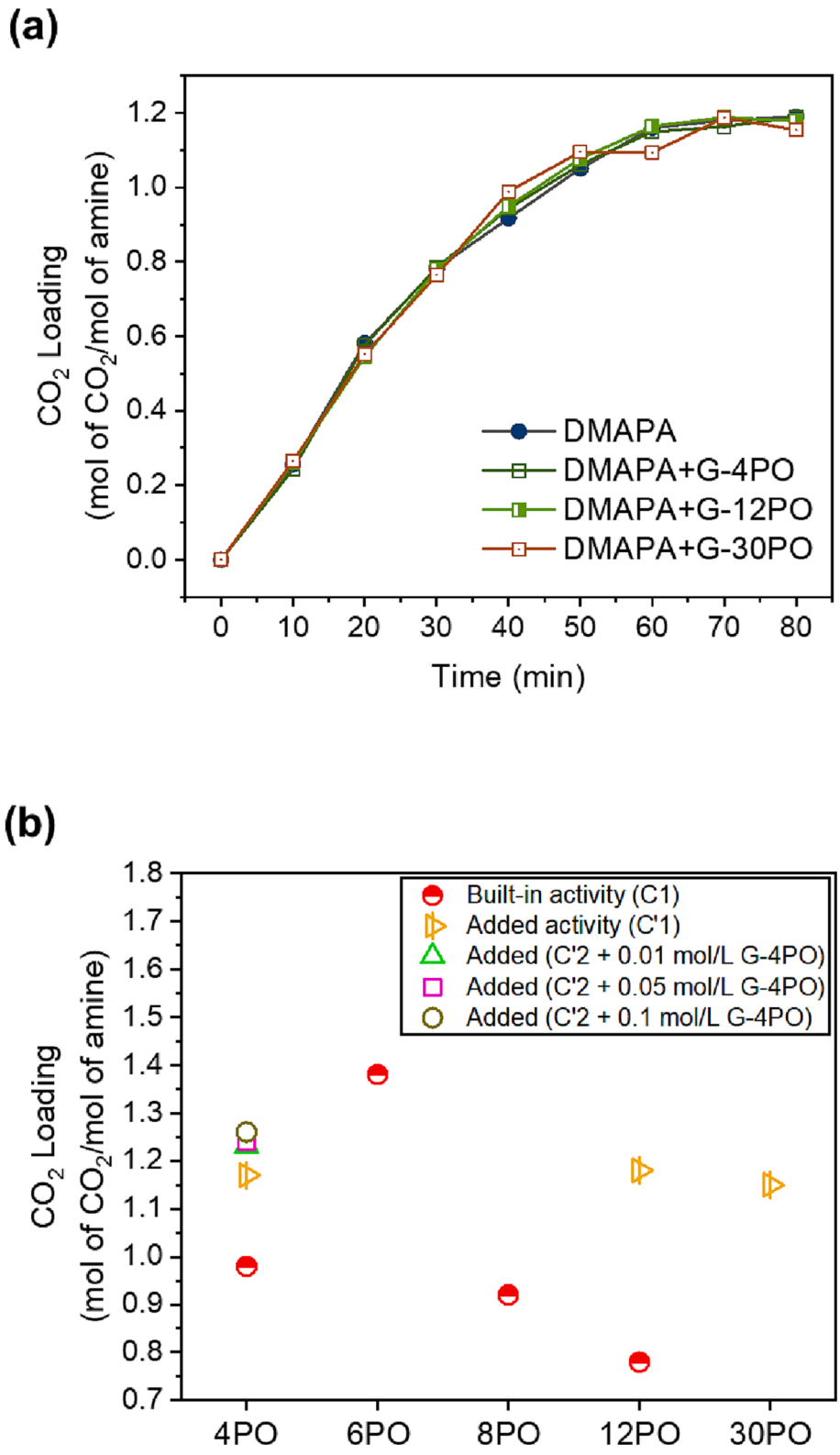

Fig. 4. (a) CO_2 loading profile of 0.116 mol/L DMAPA + 0.01 mol/L glycerol-xPO (x = 4, 12, 30), and (b) CO_2 loading overview for DMAPA + glycerol-xPO tests. *C1* is defined as 0.116 mol/L DMAPA-xPO (x = 4, 6, 8, 12) experiments; *C'1* is defined as 0.116 mol/L DMAPA + 0.01 mol/L glycerol-xPO (x = 4, 12, 30) experiments; *C'2* is defined as 0.25 mol/L DMAPA experiments.

capture ability of the amino group [27,44]. Although incorporating PO groups into DMAPA tends to reduce its surface tension to enhance CO_2 dissolution, an optimal balance between CO_2 dissolution and the chemically steric environment is required for the amino group to effectively drive the CO_2 capture reaction. Results in this research showed that this optimal balance was taken by DMAPA-6PO.

Surfactants as additives to an amine solution may promote undesirable foam formation in amine solutions, as reported in the literature [27]. However, the built-in surface activity in DMAPA-xPO samples exhibited negligible foam formation in this research likely because the

Table 2
Summarized results for the added surface activity experiments using a DMAPA + glycerol-xPO mixture.

Concentration (mol/L)	Capture solution	Surfactant	CO_2 Loading[a] (mol CO_2/mol amine)
0.116	DMAPA	None	1.18
		Glycerol 4-PO 0.01 mol/L	1.17
		Glycerol 12-PO 0.01 mol/L	1.18
		Glycerol 30-PO 0.01 mol/L	1.15
0.25	DMAPA	None	1.22
		Glycerol-4PO 0.01 mol/L	1.23
		Glycerol-4PO 0.05 mol/L	1.24
		Glycerol-4PO 0.10 mol/L	1.26

[a] STD CO_2 loading: ± 0.02.

PO group is a low foaming block [45]. Also, the PO groups at the end of the hydrocarbon chain resulted in low foaming capabilities of nonionic surfactants [45].

3.2. Built-in vs added surface activity

The effectiveness of DMAPA with the built-in surface activity (DMAPA-xPO) was compared to DMAPA with added surface activity (DMAPA + surfactant). For this purpose, glycerol-xPO (x = 4, 12, 30) was used as a surfactant additive. The glycerol-xPO samples were prepared and provided by Harcros Chemicals. The results are shown in Fig. 4. Using a 0.01 mol/L concentration of glycerol-xPO for all different levels and a 0.116 mol/L DMAPA capturing solution did not improve the CO_2 loading capacity. The maximum value was 1.18 mol of CO_2/mol of amine, and they exhibited similar histories as DMAPA (see Fig. 4a). This behavior is related to the constant CO_2 capture capacity shown at all different levels with an average value of 7.21 g/L, as illustrated in Fig. S5.

Additionally, experiments using a higher DMAPA concentration (0.25 mol/L) with a fixed PO level (glycerol-4PO) at concentrations of 0.01, 0.05, and 0.1 mol/L were carried out to evaluate the influence of the added surface activity. As can be seen in Fig. 4b, the results exhibited that no significant CO_2 loading enhancement was achieved by increasing either DMAPA concentration or glycerol-4PO concentration. Through these variations, the maximum CO_2 loading of the mixture was 1.24 mol of CO_2/mol of amine, which was only slightly higher than the 1.22 mol of CO_2/mol amine of 0.25 mol/L DMAPA. All results are listed in Table 2.

This unaffected behavior is in concordance with the literature for different types of surfactants, including nonionic and cationic ones, at different concentrations [27]. Thus, the addition of glycerol-xPO as surfactant to DMAPA solution did not affect its CO_2 capture capacity because of the limited surface activity and tendency to form micelles that tend to limit the mass transfer at the gas–liquid reaction interface [27,28]. It is reasonable to conclude that the built-in surface activity is a promising method to enhance the overall CO_2 capture capacity of an amine-based solution.

3.3. Bicarbonate production

The bicarbonate production analysis and quantification were carried out by ^{13}C NMR spectroscopy. For this purpose, the concentration of the amines used in these experiments was increased to 0.25 mol/L. The results for DMAPA are shown in Fig. 5. From the beginning of the

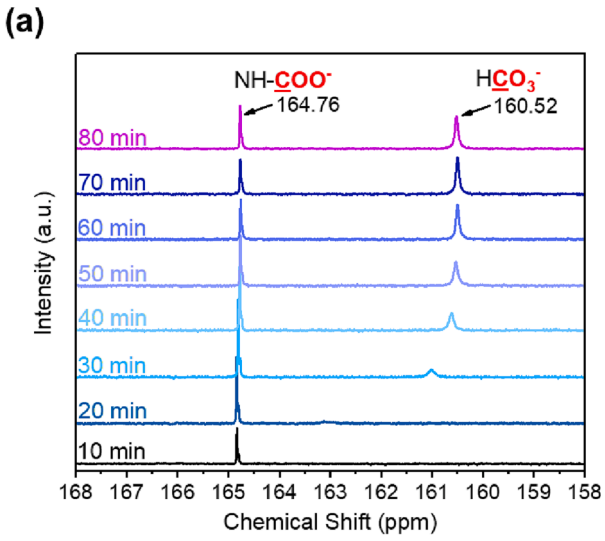

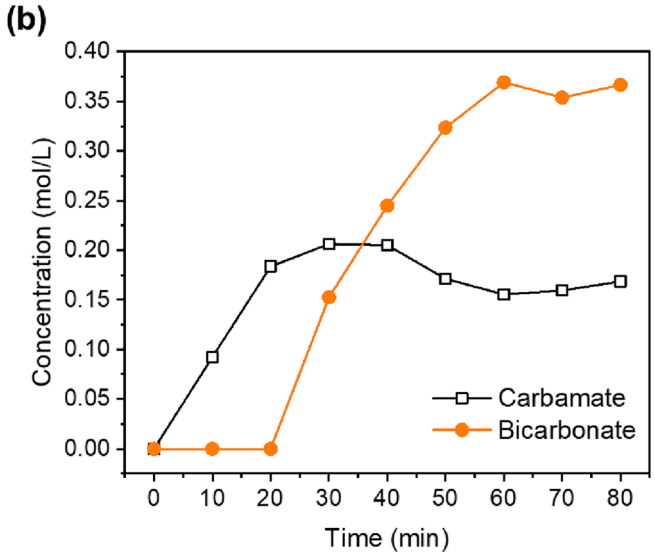

Fig. 5. (a) ^{13}C NMR spectra of 0.25 mol/L DMAPA solution during CO_2 capture; (b) Concentration profile of carbamate/bicarbonate species detected during CO_2 capture.

capture process, a signal of carbamate was detected at a chemical shift of 164.76 ppm in the ^{13}C NMR spectra as shown in Fig. 5a since DMAPA contains a primary amino group that reacts with CO_2 to form these species [22,46]. In addition, another signal at 160.52 ppm associated with bicarbonate species was observed from 30 min of reaction time because of the reaction product from the tertiary amino group and CO_2, as well as from the hydrolysis of carbamate [23,46]. These results indicated that the primary amino group in DMAPA reacted faster than the tertiary amino group. The quantification of both species during the reaction is illustrated in Fig. 5b. As it can be seen, the faster carbamate production reached its maximum at 30 min with 0.20 mol/L. From this point on, the concentration decreased until it reached a constant value of approximately 0.16 mol/L, corroborating the hydrolysis process of carbamate species. Additionally, bicarbonate generation was detected from 20 min, and it reached a constant concentration of aproximately 0.36 mol/L at 60 min of reaction. Therefore, the bicarbonate generation by DMAPA was retarded for 20 mins by the carbamate generation.

The ^{13}C NMR spectra obtained from the DMAPA-6PO are shown in Fig. 6a. A single C═O signal at 163.31 ppm was observed after 10 mins

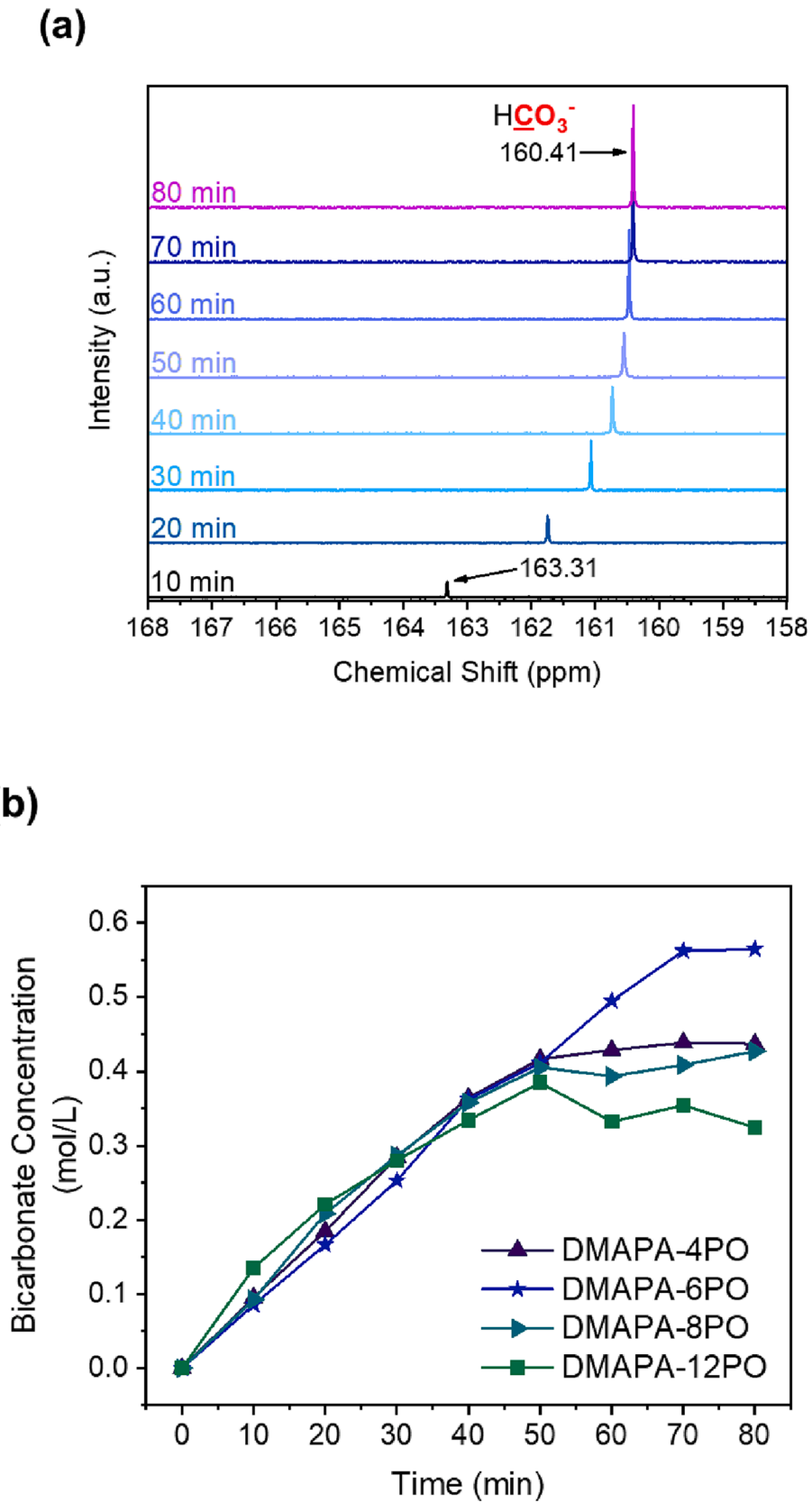

Fig. 6. (a) ^{13}C NMR spectra of 0.25 mol/L DMAPA-6PO solution during CO_2 capture; (b) Bicarbonate concentration profile during CO_2 capture.

Table 3
Summarized bicarbonate production parameters.

Sample	HCO_3^- concentration[a] (mol/L)	Time to reach the equilibrium state (min)	Average rate (mol/L•min)
DMAPA	0.3664	56.90	0.0064
DMAPA-4PO	0.4373	47.22	0.0092
DMAPA-6PO	0.5647	68.72	0.0082
DMAPA-8PO	0.4272	45.31	0.0094
DMAPA-12PO	0.3242	46.15	0.0070

[a] STD HCO_3^- concentration: ± 0.002.

of the reaction. Since the resonances of carbonate and bicarbonate species are expected at 168.5 and 160.5 ppm, respectively, this observed signal can be related to a carbonate and bicarbonate mixture in rapid equilibrium with a higher concentration of carbonate species because of the initial high pH value of the reaction (pH = 12.27) [46–48]. As the reaction continued and more CO_2 was introduced into the solution, the intensity of this signal increased and shifted to 160.41 ppm accompanied by a decrease in pH to 7.12, as evidence of a higher bicarbonate concentration. This effect can be seen in the other 4PO, 8PO, and 12PO samples presented in Fig. S6. No other signals associated with C═O for free CO_2 (124.5 ppm) or carbonic acid (156.5 ppm) were detected at any point of the reaction, suggesting a low concentration as a consequence of continuous consumption of these species [47]. In addition, the carbon signals associated with the chemical composition of DMAPA, and the surface-surface active amine including those from –CH_2–N–, –CH_3–N–, –CH_3–CH– bonds [49] were observed below 80 ppm in the full ^{13}C NMR spectra shown in Fig. S7. Therefore, the bicarbonate detection was not interfered by the presence of such compounds.

Contrary to DMAPA, the surface-active amine generated only bicarbonate species during the CO_2 capture process. The built-in surface activity by incorporating PO groups into the primary amino group of DMAPA allowed the formation of a second tertiary amino group in the molecule, preferably producing bicarbonate. However, having two tertiary amines while adding built-in surface activity was not the only booster for bicarbonate generation. The optimal PO level appeared to be the crucial factor (Fig. 6b).

DMAPA-6PO exhibited a superior performance among the different PO levels tested with a final bicarbonate concentration of 0.56 mol/L, which represents an increment in bicarbonate concentration of 54% compared with DMAPA. Fig. S8 shows the histories of bicarbonate generation for DMAPA and DMAPA-xPO. Table 3 shows the final bicarbonate concentrations, the periods required for reaching the equilibrium states, and the average rates of bicarbonate generation. Although the steric effect should be less with DMAPA-4PO than DMAPA-6PO, the CO_2 loading of DMAPA-6PO was approximately 40% greater than that of DMAPA-4PO as shown in Table 1. Likewise, DMAPA-8PO and −12PO resulted in less CO_2 loading than DMAPA-6PO. Also, these larger PO groups negatively affected the surface-active amine performance because of their steric effect [27,44].

Although DMAPA-4PO exhibited more bicarbonate generation than DMAPA, it showed less CO_2 loading capacity than DMAPA. To clarify these points, the CO_2 loading capacity/HCO_3^- generation ratio was calculated to be 3.22 for DMAPA, and 2.24 for DMAPA-4PO. It is evident that the primary amino group in DMAPA reacted with CO_2 in combination with the tertiary amino group allowing more CO_2 loading capacity. However, this primary amino group did not significantly contribute to the bicarbonate generation. The CO_2 loading capacity/HCO_3^- generation ratio for DMAPA-6PO was calculated to be 2.44, which is greater than DMAPA-4PO and explains that the optimal PO level allowed a higher bicarbonate generation ratio.

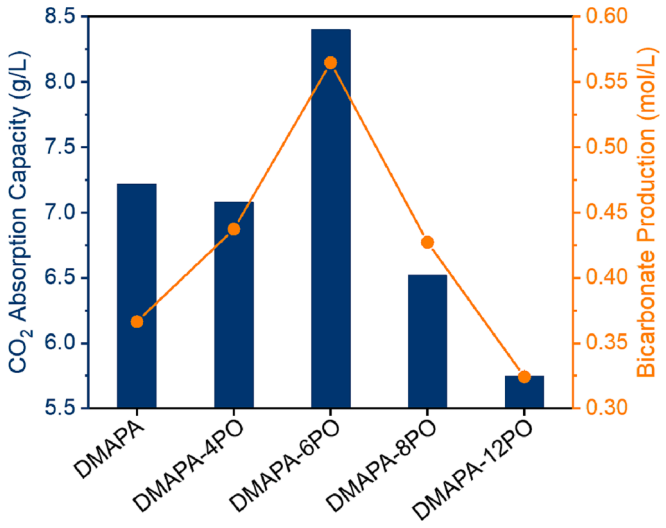

Fig. 7. Relationship between CO_2 absorption capacity and bicarbonate production for DMAPA and DMAPA-xPO (x = 4, 6, 8, 12) samples.

Overall, the incorporation of PO groups enhanced the produced bicarbonate concentration and the bicarbonate generation average rate of DMAPA. Among all DMAPA-xPO samples, DMAPA-6PO showed the longest time to reach the equilibrium state with 68.72 min while generating the greatest bicarbonate concentration. These results suggested that the optimal built-in surface activity in DMAPA-6PO enhanced the bicarbonate generation, as shown in Fig. S9. This observation can be correlated to the central role of the PO groups in the surface-active amine, allowing more CO_2 dissolution in the aqueous amine solution without taking part in the capture and *in-situ* conversion process at the nitrogen atom in the amino groups. This correlation can be appreciated in Fig. 7. The largest mass of CO_2 absorbed by the amine solution was determined to be 8.4 g/L in DMAPA-6PO, also exhibiting the highest bicarbonate concentration of 0.56 mol/L. In contrast, the lowest bicarbonate amount of 0.32 mol/L was produced by DMAPA-12PO, which also showed the smallest CO_2 absorbed mass (5.75 g/L). Thus, the built-in surface activity represents an effective pathway to enhance the overall CO_2 capture capacity, allowing more CO_2 dissolution that can efficiently be converted into bicarbonate by the tertiary amino groups.

The bicarbonate production was also evaluated at different concentrations of DMAPA-6PO surface-active amine. In addition to 0.25 mol/L as previously tested, 0.05, 0.35, and 0.4 mol/L were evaluated under the same experimental conditions. As shown in Table S2, as the surface-active amine concentration increased, the bicarbonate concentration consistently increased up to 0.88 mol/L using 0.4 mol/L DMAPA-6PO, with an average ratio of 2.17 mol of HCO_3^-/mol of amine, while the average CO_2 loading ratio was constant around 1.30 mol of CO_2/mol of amine. These results corroborated the remarkable performance of DMAPA-6PO for bicarbonate production while capturing CO_2.

The proposed pathways for CO_2 capture and *in-situ* conversion into bicarbonate are presented in Fig. 8. Initially, CO_2 gas is dissolved in water which acts as a nucleophile (Lewis base) to produce carbonic acid at a low concentration (Fig. 8a). Then, the surface-active amine takes place as a proton acceptor (Bronsted base) and reacts with CO_2 in the form of carbonic acid, producing an equilibrium state between carbonate and bicarbonate, and protonated amine (Fig. 8b). As the protonation of the surface-active amine increases, the basicity of the amine is consumed and the pH decreases, favoring the bicarbonate production. Along with this pH reduction, carbonate can also deprotonate carbonic acid to produce bicarbonate as a simultaneous reaction (Fig. 8c). Note also that these CO_2 reaction pathways could occur simultaneously at the second nitrogen in the DMAPA-xPO molecule. However, the

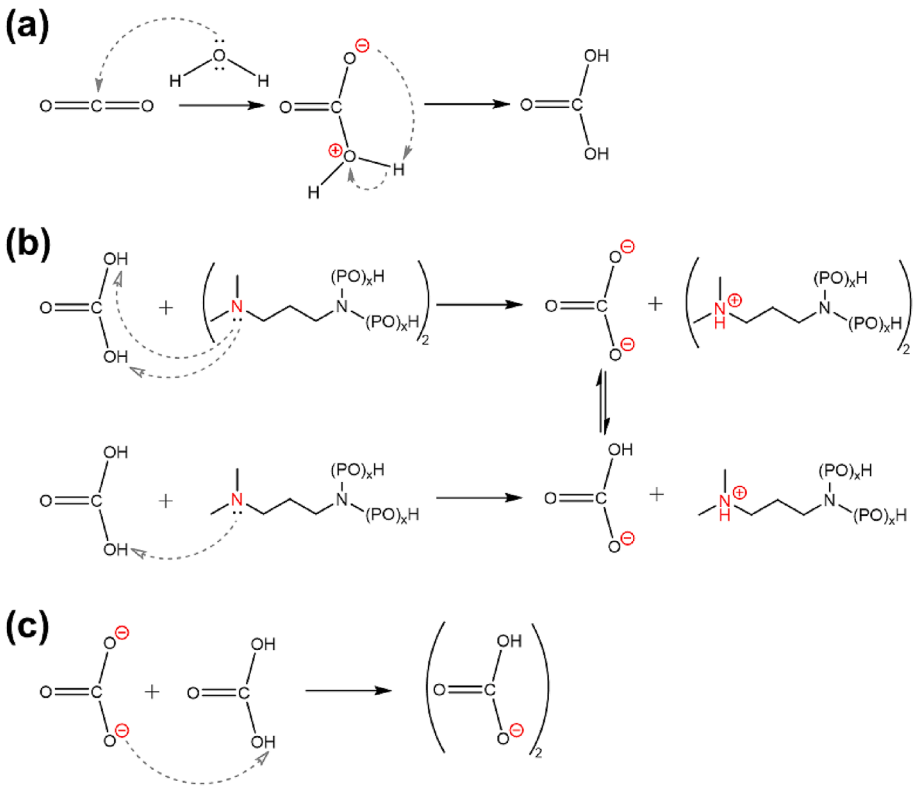

Fig. 8. Proposed pathways for CO_2 reaction with DMAPA-xPO in aqueous solution: (a) CO_2 dissolution into H_2CO_3 in aqueous phase; (b) DMAPA-xPO reaction with H_2CO_3 to produce HCO_3^-; and (c) H_2CO_3 deprotonation to form HCO_3^-.

Table 4
Comparative table of different CO_2 capture systems and their performances.

No.	Capture system	Amine capture solution	Added surfactant	CO_2 loading (mol CO_2/mol amine)	CO_2 capture experimental conditions	HCO_3^- generation (mol HCO_3^-/mol amine)	Reference
1	Single amine	MEA (30 wt%)	None	0.56	1 L CO_2/min 40–80 °C	No reported	[53]
2		AMP (30 wt%)	None	0.86		No reported	
3	Single amine	DMAPA (1 mol/L)	None	1.02	15 vol% CO_2 25 °C	No reported	[41]
4	Amine solution mixture	DMAPA-NHD-H_2O	None	1.06	12.5 vol% CO_2 40 °C	No reported	[37]
5	Amine + surfactant	MEA (30 wt%)	Triton X100 (0.28 mmol/L)	0.55	95 mL CO_2/min 40 °C	No reported	[27]
6			CTAB (0.96 mmol/L)	0.60		No reported	
7	Built-in surface active amine	DMAPA-6PO (0.116 mol/L)	None	1.38	50 mL CO_2/min Room temp. Ambient pressure	2.17	This research

investigation into mechanisms with the multiple performing nitrogen sites, as well as their production ratio, is out of the scope of this paper. The PO groups and the amino groups play different roles in enhancing the overall bicarbonate generation.

The cost-competitiveness analysis of this bicarbonate pathway must include CO_2 capture as bicarbonate, bicarbonate/surface-active amine separation by a membrane, and the surface-active amine regeneration by deprotonation, among many other factors. That scenario also includes the bicarbonate conversion into formate/formic acid by electrolysis. Such analysis will be performed in the next phase of research considering different parameters, such as the energy consumption for solvent regeneration (conventional CO_2 capture using MEA around 3.5–3.8 GJ/ton CO_2) [50–52].

Nevertheless, Table 4 presents a comparison between CO_2 capture as bicarbonate and conventional CO_2 capture. It shows that the built-in surface activity of DMAPA-6PO exhibited superior CO_2 loading performance in comparison to different systems composed of single amines, amine solution mixture, and amine + surfactant. The bicarbonate generation was proposed and studied for the first time in this research as an alternative to conventional CO_2 capture technologies.

4. Conclusions

We demonstrated the technical feasibility of CO_2 capture and *in-situ*

conversion into bicarbonate by using DMAPA with the built-in surface activity by PO-group incorporation that enhanced the bicarbonate generation. The CO_2 capture experiments under ambient conditions and ^{13}C NMR spectroscopy analyses revealed that the built-in surface activity enhanced CO_2 solubilization in the aqueous amine solution, improving the CO_2 capture and conversion into bicarbonate. Using an optimal PO incorporation (DMAPA-6PO), the bicarbonate generation was improved by 54% compared to DMAPA without the built-in surface activity. CO_2 capture as bicarbonate as studied in this research can be integrated with electrochemical conversion into green carbon chemicals, such as formic acid, toward carbon neutrality in the energy transition.

CRediT authorship contribution statement

Omar A. Carrasco-Jaim: Methodology, Validation, Formal analysis, Investigation, Data curation, Writing – original draft, Visualization. **Haojun Xia:** Validation, Formal analysis, Investigation, Data curation, Writing – original draft, Visualization. **Upali P. Weerasooriya:** Methodology, Validation, Formal analysis, Resources. **Ryosuke Okuno:** Conceptualization, Methodology, Validation, Formal analysis, Resources, Writing – review & editing, Supervision, Project administration, Funding acquisition.

Declaration of Competing Interest

The authors declare that they have no known competing financial interests or personal relationships that could have appeared to influence the work reported in this paper.

Data availability

Data will be made available on request.

Acknowledgements

We acknowledge sponsors of the Energi Simulation Industrial Affiliate Program on Carbon Utilization and Storage (ES Carbon UT) at the Center for Subsurface Energy and the Environment at The University of Texas at Austin. Ryosuke Okuno holds the Pioneer Corporation Faculty Fellowship in Petroleum Engineering at the University of Texas at Austin. We also acknowledge Harcros Chemicals Inc. for the assistance in preparing various chemical samples used in this research.

Appendix A. Supplementary data

Supplementary data to this article can be found online at https://doi.org/10.1016/j.fuel.2023.128554.

References

[1] Liu Z, Deng Z, Davis SJ, Giron C, Ciais P. Monitoring global carbon emissions in 2021. Nat Rev Earth Environ 2022;3:217–9. https://doi.org/10.1038/s43017-022-00285-w.
[2] Wang X, Song C. Carbon Capture From Flue Gas and the Atmosphere: A Perspective. Front Energy Res 2020;8. 10.3389/fenrg.2020.560849.
[3] Ghiat I, Al-Ansari T. A review of carbon capture and utilisation as a CO_2 abatement opportunity within the EWF nexus. J CO_2 Util 2021;45:101432.
[4] Okoye-Chine CG, Otun K, Shiba N, Rashama C, Ugwu SN, Onyeaka H, et al. Conversion of carbon dioxide into fuels – A review. J CO_2 Util 2022;62:102099.
[5] Rochelle GT. Conventional amine scrubbing for CO_2 capture. Absorption-Based Post-Combustion Capture of Carbon Dioxide, Elsevier Inc.; 2016, p. 35–67. 10.1016/B978-0-08-100514-9.00003-2.
[6] Wall TF. Combustion processes for carbon capture. Proc Combust Inst 2007;31:31–47. https://doi.org/10.1016/j.proci.2006.08.123.
[7] Raganati F, Miccio F, Ammendola P. Adsorption of Carbon Dioxide for Post-combustion Capture: A Review. Energy Fuel 2021;35:12845–68. https://doi.org/10.1021/acs.energyfuels.1c01618.
[8] Gutiérrez-Sánchez O, Bohlen B, Daems N, Bulut M, Pant D, Breugelmans T. A State-of-the-Art Update on Integrated CO_2 Capture and Electrochemical Conversion Systems. ChemElectroChem 2022;9. https://doi.org/10.1002/celc.202101540.
[9] Wu H, Li Q, Zhang Y, Qiu M, Liao Y, Xu H, et al. One-step supramolecular fabrication of ionic liquid/ZIF-8 nanocomposites for low-energy CO_2 capture from flue gas and conversion. Fuel 2022;322:124175.
[10] Stanton Ribeiro M, Zanatta M, Corvo MC. Ionic liquids and biomass as carbon precursors: Synergistically answering a call for CO_2 capture and conversion. Fuel 2022;327:125164.
[11] Aghel B, Janati S, Wongwises S, Shadloo MS. Review on CO_2 capture by blended amine solutions. Int J Greenh Gas Control 2022;119:103715. https://doi.org/10.1016/j.ijggc.2022.103715.
[12] Bui M, Adjiman CS, Bardow A, Anthony EJ, Boston A, Brown S, et al. Carbon capture and storage (CCS): The way forward. Energy Environ Sci 2018;11(5):1062–176.
[13] Liang Z(, Rongwong W, Liu H, Fu K, Gao H, Cao F, et al. Recent progress and new developments in post-combustion carbon-capture technology with amine based solvents. Int J Greenh Gas Control 2015;40:26–54.
[14] Wu SY, Liu YF, Chu CY, Li YC, Liu CM. Optimal absorbent evaluation for the CO_2 separating process by absorption loading, desorption efficiency, cost, and environmental tolerance. Int J Green Energy 2015;12:1025–30. https://doi.org/10.1080/15435075.2014.910781.
[15] Gautam A, Kumar MM. Post-combustion capture of CO_2 using novel aqueous Triethylenetetramine and 2-Dimethylaminoethanol amine blend: Equilibrium CO_2 loading-empirical model and optimization, CO_2 desorption, absorption heat, and ^{13}C NMR analysis. Fuel 2023;331:125864. https://doi.org/10.1016/j.fuel.2022.125864.
[16] Li T, Lees EW, Goldman M, Salvatore DA, Weekes DM, Berlinguette CP. Electrolytic Conversion of Bicarbonate into CO in a Flow Cell. Joule 2019;3:1487–97. https://doi.org/10.1016/j.joule.2019.05.021.
[17] Welch AJ, Dunn E, Duchene JS, Atwater HA. Bicarbonate or Carbonate Processes for Coupling Carbon Dioxide Capture and Electrochemical Conversion. ACS Energy Lett 2020;5:940–5. https://doi.org/10.1021/acsenergylett.0c00234.
[18] Chowdhury FA, Yamada H, Higashii T, Goto K, Onoda M. CO_2 capture by tertiary amine absorbents: A performance comparison study. Ind Eng Chem Res 2013;52:8323–31. https://doi.org/10.1021/ie400825u.
[19] Bernhardsen IM, Knuutila HK. A review of potential amine solvents for CO_2 absorption process: Absorption capacity, cyclic capacity and pKa. Int J Greenh Gas Control 2017;61:27–48. https://doi.org/10.1016/j.ijggc.2017.03.021.
[20] Putta KR, Svendsen HF, Knuutila HK. Kinetics of CO_2 Absorption in to Aqueous MEA Solutions Near Equilibrium. Energy Proc 2017;114:1576–83.
[21] Mohamed Mohsin H, Mohd Shariff A, Johari K. 3-Dimethylaminopropylamine (DMAPA) mixed with glycine (GLY) as an absorbent for carbon dioxide capture and subsequent utilization. Sep Purif Technol 2019;222:297–308. https://doi.org/10.1016/j.seppur.2019.04.029.
[22] Nath D, Henni A. Solubility of carbon dioxide (CO_2) in aqueous solution of 3-(dimethylamino)-1-propylamine (DMAPA). Fluid Phase Equilib 2020;511:112506. https://doi.org/10.1016/j.fluid.2020.112506.
[23] Zhang R, Yang Q, Yu B, Yu H, Liang Z. Toward to efficient CO_2 capture solvent design by analyzing the effect of substituent type connected to N-atom. Energy 2018;144:1064–72. https://doi.org/10.1016/j.energy.2017.12.095.
[24] Bajwa GS, Sammon C, Timmins P, Melia CD. Molecular and mechanical properties of hydroxypropyl methylcellulose solutions during the sol:gel transition. Polymer (Guildf) 2009;50:4571–6. https://doi.org/10.1016/j.polymer.2009.06.075.
[25] Kanokkarn P, Shiina T, Santikunaporn M, Chavadej S. Equilibrium and dynamic surface tension in relation to diffusivity and foaming properties: Effects of surfactant type and structure. Colloids Surf A 2017;524:135–42. https://doi.org/10.1016/j.colsurfa.2017.04.043.
[26] Nascimento AEG, Barros Neto EL, Moura MCPA, Castro Dantas TN, Dantas Neto AA. Wettability of paraffin surfaces by nonionic surfactants: Evaluation of surface roughness and nonylphenol ethoxylation degree. Colloids Surf A 2015;480:376–83. https://doi.org/10.1016/j.colsurfa.2014.11.003.
[27] Pichetwanit P, Kungsanant S, Supap T. Effects of surfactant type and structure on properties of amines for carbon dioxide capture. Colloids Surf A 2021;622:126602. https://doi.org/10.1016/j.colsurfa.2021.126602.
[28] Bryant JJ, Lippert C, Qi G, Liu K, Mannel DS, Liu K. Enhanced Carbon Capture through Incorporation of Surfactant Additives. Ind Eng Chem Res 2016;55:7456–61. https://doi.org/10.1021/acs.iecr.5b04906.
[29] Mohammadpour A, Mirzaei M, Azimi A, Tabatabaei Ghomsheh SM. Solubility and absorption rate of CO_2 in MEA in the presence of graphene oxide nanoparticle and sodium dodecyl sulfate. Int J Ind Chem 2019;10:205–12. https://doi.org/10.1007/s40090-019-0184-5.
[30] Han S, Jeon S-i, Lee J, Ahn J, Lee C, Lee J, et al. Efficient bicarbonate removal and recovery of ammonium bicarbonate as CO_2 utilization using flow-electrode capacitive deionization. Chem Eng J 2022;431:134233.
[31] Wang DX, Wang XL, Tomi Y, Ando M, Shintani T. Modeling the separation performance of nanofiltration membranes for the mixed salts solution. J Memb Sci 2006;280:734–43. https://doi.org/10.1016/j.memsci.2006.02.032.
[32] Lee G, Li YC, Kim J-Y, Peng T, Nam D-H, Sedighian Rasouli A, et al. Electrochemical upgrade of CO_2 from amine capture solution. Nat Energy 2021;6(1):46–53.
[33] Pérez-Gallent E, Vankani C, Sánchez-Martínez C, Anastasopol A, Goetheer E. Integrating CO_2 capture with electrochemical conversion using amine-based capture solvents as electrolytes. Ind Eng Chem Res 2021;60:4269–78. https://doi.org/10.1021/acs.iecr.0c05848.

[34] Bhattacharya M, Sebghati S, Vercella YM, Saouma CT. Electrochemical Reduction of Carbamates and Carbamic Acids: Implications for Combined Carbon Capture and Electrochemical CO2 Recycling. J Electrochem Soc 2020;167(8):086507.
[35] Chen Lu, Li F, Zhang Y, Bentley CL, Horne M, Bond AM, et al. Electrochemical Reduction of Carbon Dioxide in a Monoethanolamine Capture Medium. ChemSusChem 2017;10(20):4109–18.
[36] Norouzbahari S, Shahhosseini S, Ghaemi A. Chemical absorption of CO_2 into an aqueous piperazine (PZ) solution: Development and validation of a rigorous dynamic rate-based model. RSC Adv 2016;6:40017–32. https://doi.org/10.1039/c5ra27869d.
[37] Qiu Y, Lu H, Zhu Y, Liu Y, Wu K, Liang B. Phase-Change CO_2 Absorption Using Novel 3-Dimethylaminopropylamine with Primary and Tertiary Amino Groups. Ind Eng Chem Res 2020;59:8902–10. https://doi.org/10.1021/acs.iecr.9b06886.
[38] Wang X, Akhmedov NG, Duan Y, Li B. Nuclear magnetic resonance studies of CO_2 absorption and desorption in aqueous sodium salt of alanine. Energy Fuel 2015;29:3780–4. https://doi.org/10.1021/acs.energyfuels.5b00535.
[39] Vaidya PD, Kenig EY. CO_2-alkanolamine reaction kinetics: A review of recent studies. Chem Eng Technol 2007;30:1467–74. https://doi.org/10.1002/ceat.200700268.
[40] Donaldson TL, Nguyen YN. Carbon Dioxide Reaction Kinetics and Transport in Aqueous Amine Membranes. Ind Eng Chem Fundam 1980;19:260–6. https://doi.org/10.1021/i160075a005.
[41] Chen Y, Jiang W, Luo X, Huang Y, Jin Bo, Gao H, et al. The study of kinetics of CO_2 absorption into 3-dimethylaminopropylamine and 3-diethylaminopropylamine aqueous solution. Int J Greenh Gas Control 2018;75:214–23.
[42] Nath D, Henni A. Kinetics of carbon dioxide (CO_2) with 3-(dimethylamino)-1-propylamine in water and methanol systems using the stopped-flow technique. Ind Eng Chem Res 2020;59:14625–35. https://doi.org/10.1021/acs.iecr.0c01157.
[43] Karunarathne SS, Eimer DA, Øi LE. Physical Properties of MEA + Water + CO_2 Mixtures in Postcombustion CO_2 Capture: A Review of Correlations and Experimental Studies. J Eng (United Kingdom) 2020; 2020.. https://doi.org/10.1155/2020/7051368.
[44] Conway W, Wang X, Fernandes D, Burns R, Lawrance G, Puxty G, et al. Toward the understanding of chemical absorption processes for post-combustion capture of carbon dioxide: Electronic and steric considerations from the kinetics of reactions of CO_2(aq) with sterically hindered amines. Environ Sci Technol 2013;47(2):1163–9.
[45] Polito A, Folli A, Breitzke B. Multi-purpose surfactants: Low-foaming, fast wetting and biodegradable C11 oxo alcohol alkoxylates. Riv Ital Delle Sostanze Grasse 2008;85:60–6.
[46] Lv B, Guo B, Zhou Z, Jing G. Mechanisms of CO_2 Capture into Monoethanolamine Solution with Different CO_2 Loading during the Absorption/Desorption Processes. Environ Sci Technol 2015;49:10728–35. https://doi.org/10.1021/acs.est.5b02356.
[47] Kortunov PV, Siskin M, Baugh LS, Calabro DC. In Situ Nuclear Magnetic Resonance Mechanistic Studies of Carbon Dioxide Reactions with Liquid Amines in Aqueous Systems: New Insights on Carbon Capture Reaction Pathways. Energy Fuel 2015;29:5919–39. https://doi.org/10.1021/acs.energyfuels.5b00850.
[48] Kortunov PV, Siskin M, Paccagnini M, Thomann H. CO_2 Reaction Mechanisms with Hindered Alkanolamines: Control and Promotion of Reaction Pathways. Energy Fuel 2016;30:1223–36. https://doi.org/10.1021/acs.energyfuels.5b02582.
[49] Yu B, Yu H, Yang Qi, Li K, Ji L, Zhang R, et al. Postcombustion Capture of CO_2 by Diamines Containing One Primary and One Tertiary Amino Group: Reaction Rate and Mechanism. Energy Fuel 2019;33(8):7500–8.
[50] Gutiérrez-Sánchez O, Bohlen B, Daems N, Bulut M, Pant D, Breugelmans T. A State-of-the-Art Update on Integrated CO_2 Capture and Electrochemical Conversion Systems. ChemElectroChem 2022;9:e202101540.
[51] Sakwattanapong R, Aroonwilas A, Veawab A. Behavior of reboiler heat duty for CO_2 capture plants using regenerable single and blended alkanolamines. Ind Eng Chem Res 2005;44:4465–73. https://doi.org/10.1021/ie050063w.
[52] Zheng RF, Barpaga D, Mathias PM, Malhotra D, Koech PK, Jiang Y, et al. A single-component water-lean post-combustion CO_2 capture solvent with exceptionally low operational heat and total costs of capture – comprehensive experimental and theoretical evaluation. Energy Environ Sci 2020;13(11):4106–13.
[53] Kim YE, Lim JA, Jeong SK, Yoon YI, Bae ST, Nam SC. Comparison of carbon dioxide absorption in aqueous MEA, DEA, TEA, and AMP solutions. Bull Korean Chem Soc 2013;34(3):783–7.